Myung Gwan Hahm
Department of Mechanical and Industrial Engineering,
NSF Nanoscale Science and Engineering Center for High-Rate Nanomanufacturing,
Northeastern University,
Boston, MA 02115
e-mail: mghahm@coe.neu.edu

Young-Kyun Kwon
e-mail: ykkwon@khu.ac.kr
Department of Physics and Research Institute for Basic Sciences,
Kyung Hee University,
Seoul 130-701, Korea

Ahmed Busnaina

Yung Joon Jung[1]
e-mail: jungy@coe.neu.edu

Department of Mechanical and Industrial Engineering,
NSF Nanoscale Science and Engineering Center for High-Rate Nanomanufacturing,
Northeastern University,
Boston, MA 02115

Structure Controlled Synthesis of Vertically Aligned Carbon Nanotubes Using Thermal Chemical Vapor Deposition Process

Due to their unique one-dimensional nanostructure along with excellent mechanical, electrical, and optical properties, carbon nanotubes (CNTs) become a promising material for diverse nanotechnology applications. However, large-scale and structure controlled synthesis of CNTs still have many difficulties due to the lack of understanding of the fundamental growth mechanism of CNTs, as well as the difficulty of controlling atomic-scale physical and chemical reactions during the nanotube growth process. Especially, controlling the number of graphene wall, diameter, and chirality of CNTs are the most important issues that need to be solved to harness the full potential of CNTs. Here we report the large-scale selective synthesis of vertically aligned single walled carbon nanotubes (SWNTs) and double walled carbon nanotubes (DWNTs) by controlling the size of catalyst nanoparticles in the highly effective oxygen assisted thermal chemical vapor deposition (CVD) process. We also demonstrate a simple but powerful strategy for synthesizing ultrahigh density and diameter selected vertically aligned SWNTs through the precise control of carbon flow during a thermal CVD process. [DOI: 10.1115/1.4002443]

1 Introduction

Nanotechnologies based on carbon nanotubes (CNTs) are developed very rapidly from the discovery in 1993 [1] because of their exceptional mechanical, electrical, and optical properties [2]. The applications of CNTs are their use in nanoscale electronics such as nanosensors, interconnects, and field effect transistors by their specific electronic structures, superior transport properties, and unique one-dimensional nanostructures [3–5]. In the synthesis of CNTs, the catalytic chemical vapor deposition (CVD) method has been developed actively for the large-scale synthesis of CNTs [6–12]. However, still challenging difficulties are the control of morphology and structure of CNTs with the ability of synthesizing them in a large quantity. The key parameters in CNT growth using thermal CVD processes are chemical and physical characteristics of catalyst nanoparticles, hydrocarbons, and reaction environment during growth of CNTs. In the CVD process, the dissociation of hydrocarbon molecules catalyzed by the transition metal and the precipitation of sp^2 carbon bonds from supersaturated metal catalyst nanoparticles lead to the formation of CNTs. Therefore, the diameter of CNTs is closely related to the size of metal catalyst nanoparticles. However, it is very difficult to control the size of catalyst nanoparticles precisely with the uniform distribution. In this paper, we report the large-scale selective growth of vertically aligned (VA) SWNTs and DWNTs using an ethanol based thermal CVD process. We also demonstrate the large-scale synthesis of diameter controlled vertically aligned SWNTs by controlling the flow rate of ethanol vapor. To understand the diameter selected growth of SWNTs, we also carried out a computational investigation of the fundamental SWNT growth mechanism and kinetics under different ethanol flow rates in the CVD process using various computational techniques, including the first-principles formalism.

2 Experimental Method

Vertically aligned CNTs were synthesized by employing a thermal ethanol CVD technique [13]. Figure 1 is a schematic showing our ethanol CVD system and experimental procedure for the growth of high density and vertically aligned CNTs. First, a 20 nm thick Al film was deposited onto a SiO_2 layer using a sputter coater and exposed to the air for the formation of aluminum-oxide buffer layer to grow highly dense and vertically aligned CNTs (Fig. 1(*b*)). Then, an ultrathin Co catalyst film with 0.5–1 nm thickness was deposited on an Al_2O_x/SiO_2 multilayer using an e-beam evaporator (Fig. 1(*c*)). The prepared substrate ($Co/Al_2O_x/SiO_2$) was placed inside of a quartz tube and the CVD chamber was evacuated to 15 mTorr. Then the temperature was increased to 850°C while being exposed to an argon-hydrogen mixture gas (5% hydrogen balanced Ar) with 100 SCCM (SCCM denotes cubic centimeter per minute at STP) flow rate. In a desired reaction temperature (850°C), controlled high purity anhydrous ethanol (99.95%) was supplied as a carbon source for the high density nucleation and growth of CNTs resulting in vertically aligned CNT arrays (Fig. 1(*d*)). For the characterization of the CNT structure and morphology, transmission electron microscope (TEM), Raman spectroscopy, and scanning electron microscopy (SEM) were used. Especially, to investigate the large-scale diameter distribution of synthesized vertically aligned SWNTs, a Raman radial breathing mode (RBM) mapping process was employed with an excitation wavelength at 785 nm. Raman RBM maps were recorded using a Raman microscope (LabRAM HR 800, HORIBA Jobin Yvon) and a mechanical-optical mapping stage.

3 Results and Discussion

Figure 2(*a*) shows a cross-sectional optical image of CNT film grown using an ethanol CVD process. During the CVD reaction, controlled amounts of oxygen in ethanol molecules (C_2H_5OH) work as a weak oxidizer that would selectively remove amor-

[1]Corresponding author.
Manuscript received June 15, 2009; final manuscript received January 13, 2010; published online November 15, 2010. Assoc. Editor Wilson K. S. Chiu.

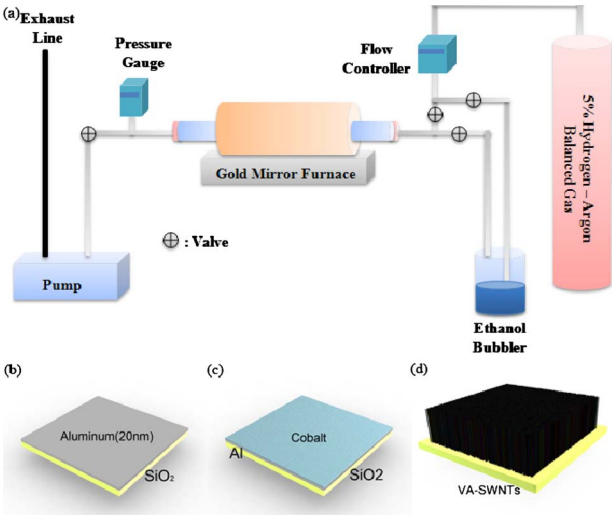

Fig. 1 Schematics of ethanol CVD systems and experimental procedures for the growth of vertically aligned SWNT

phous carbon around catalyst nanoparticles but would not damage CNTs, thereby enhancing the activity and lifetime of catalyst nanoparticles [14,15]. In our result, it is clearly seen that CNTs are vertically aligned due to the high density nucleation and growth in a highly effective ethanol CVD process. The height of vertically aligned CNT film is about 2.3 mm with the 90 min growth time. Under the same CVD parameters such as catalyst system, growth temperature, pressure, and the amount of carbon source, the height of aligned CNTs could be tailored in the range 20–2500 μm by controlling the growth time. Figures 2(*b*) and 2(*c*) show the representative SEM images of highly dense and vertically aligned SWNTs and microsized line blocks of them. Assembling CNTs into macro-/microscale architectures having vertical orientation

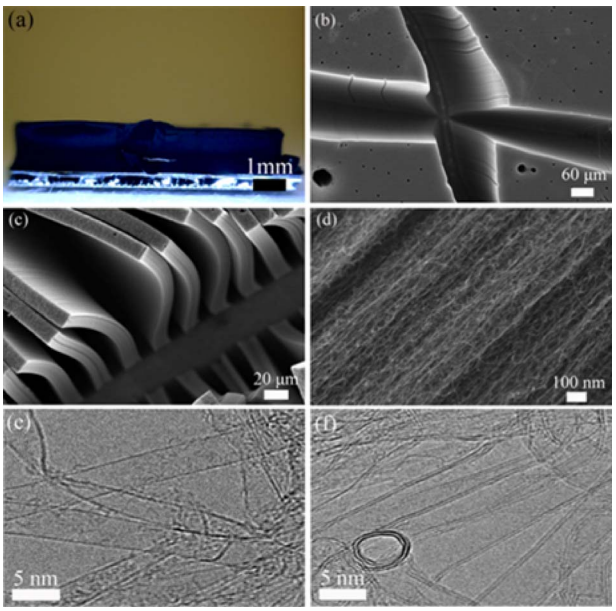

Fig. 2 (*a*) A cross-sectional optical image of highly dense and vertically aligned SWNTs grown with ethanol vapor as a carbon source, (*b*) low magnification SEM image of vertically aligned SWNTs, (*c*) low magnification SEM image of vertically aligned SWNT microblocks, (*d*) high magnification SEM image showing aligned nature of SWNTs grown in a thermal ethanol CVD process, high-resolution TEM images showing selectively synthesized (*e*) SWNTs and(*f*) DWNTs

and diverse configurations can be performed by combining conventional microfabrication techniques and the CVD process described above. For this, first, the photoresist film was spin coated and patterned on the silicon substrate using an optical lithography process. After that, the Co catalyst film (5–10 Å) was deposited and followed by photoresist lift-off process resulting in patterned catalyst film on the substrate. Then, an ethanol CVD process was conducted to create a vertically aligned and highly organized CNT architecture. Figure 2(*d*) is a high magnification SEM image indicating the aligned nature of SWNT film.

For the selective synthesis of vertically aligned SWNTs and DWNTs, different thicknesses and deposition rates of a Co catalyst film were used. For example, in order to grow SWNTs, the deposition rate of a Co catalyst film was 1 Å/s for 3 s. For the growth of DWNTs, the Co catalyst film was deposited with 3 Å/s deposition rate for 3 s. When a thicker Co catalyst film (1 nm) was deposited and used, relatively larger Co catalyst nanoparticles (4–7 nm) were formed during CVD reaction resulting in the growth of DWNTs. However, thinner Co catalyst films (0.3–0.5 nm) are directly formed into smaller catalyst nanoparticles (1–4 nm) during high temperature CVD process that can effectively prompt the growth of SWNTs on the substrate [13]. HRTEM images (Figs. 2(*e*) and 2(*f*)) show selective growth of SWNTs and DWNTs, respectively, using our controlled catalyst nanoparticle systems. From the HRTEM characterization, we also confirmed that multiwalled carbon nanotubes (MWNTs) were rarely formed in our CNT growth process.

To control the diameter of vertically aligned SWNTs, we have controlled the flow rate of ethanol (carbon source for the growth of SWNTs) while maintaining all other CVD parameters such as the size distribution of catalyst nanoparticles, temperature, pressure, and CVD process time and constant. Figure 3(*a*) shows the typical G and D band Raman spectra from SWNTs grown with 50 SCCM and 200 SCCM ethanol flow rate, respectively. G band is in a spectral range of 1550–1600 cm^{-1} identified with the tangential stretch of graphene structure. The disorder induced D band mode is at 1300 cm^{-1}. Using the peak intensity of D (I_D) and G (I_G) bands, we can determine the degree of disorder in CNT. The I_D/I_G ratio of vertically aligned SWNTs synthesized with 50 SCCM and 200 SCCM flow rates are 0.14 and 0.15, respectively. It shows that our synthesized SWNTs have very small amounts of defects, indicating that our ethanol CVD process is very effective in growing high quality SWNTs. In order to investigate the large area diameter distribution of vertically aligned SWNTs, we have used the Raman mapping process and imaging of the RBM region (the spectral range of 100–450 cm^{-1}) with its high spatial resolution. Raman maps were recorded with a mapping stage and a 785 nm excitation laser. The Raman mapping area was 10×10 μm^2 with 0.4 μm laser steps. The beam exposure time was 4 s/spectrum, and the number of accumulation is 12 for one Raman spectrum. The diameter of the confocal hole was set to 200 μm, a 600 grooves/mm grating was used, and the objective lens is 100×. The maps were recorded in standard point mapping mode with a 0.4 μm step, resulting in 625 spectra ($=25 \times 25$ spectra) and the data normalized to unit area. Figure 3(*b*) shows a representative RBM spectrum of high density and vertically aligned SWNTs after the mapping process on 10×10 μm^2. The RBM modes correspond to the atomic vibration of carbon atoms in the radial direction that allows us to calculate the diameter of SWNTs using the following equation: $\omega_{RBM}=A/d_t+B$ [16], where A and B are the proportional constants determined experimentally. For the typical SWNT bundles, A is 234 cm^{-1} nm and B is 10 cm^{-1}, where B is a blue-shift coming from a nanotube-nanotube interaction [16]. Three major RBM peak positions (three highest intensities in RBM) of Raman RBM map recorded from SWNTs grown with 50 SCCM flow rate of ethanol are 211 cm^{-1}, 230 cm^{-1}, and 303 cm^{-1} (Fig. 3(*b*)). A multivariate analysis algorithm was applied in an unsupervised mode to extract significant different spectra and to calculate cores of individual spectra.

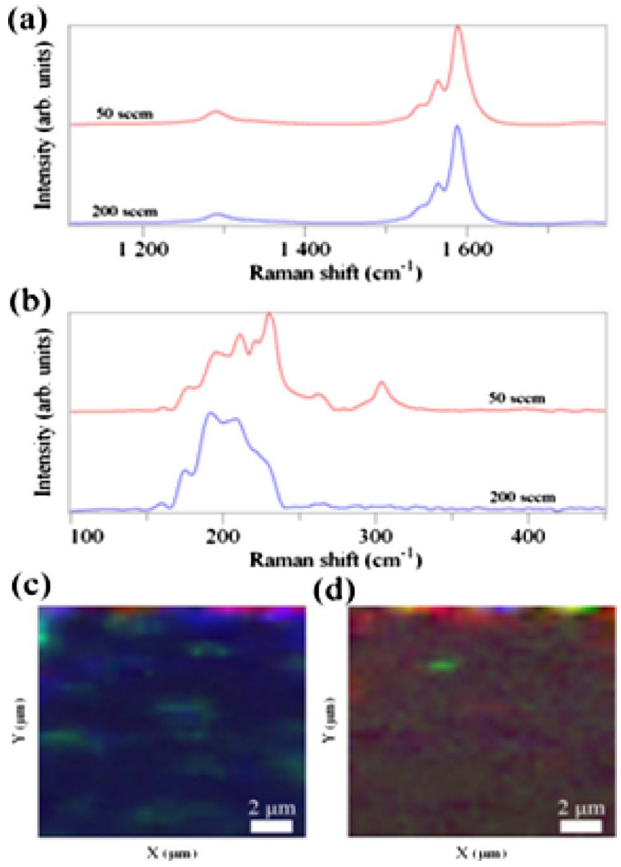

Fig. 3 (*a*) **D, G band spectra of vertically aligned SWNTs grown with 50 SCCM (red) and 200 SCCM (blue) flow rates of ethanol;** (*b*) **representative RBM spectra of vertically aligned SWNTs synthesized with 50 SCCM and 200 SCCM ethanol flow rates extracted from RBM mapping process, Raman RBM hyperspectral images from SWNTs grown with** (*c*) **50 SCCM and** (*d*) **200 SCCM;** (*c*) **the spatial diameter distribution of VA-SWNTs grown with 50 SCCM flow rate of ethanol is very uniform (blue color occupied 93% of the entire SWNT film);** (*d*) **the RBM image showing wide diameter distribution of vertically aligned SWNTs grown with 200 SCCM**

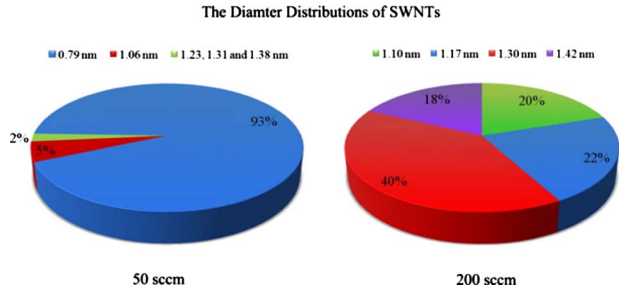

Fig. 4 The charts of the major diameter distribution of VA-SWNTs grown with two different flow rates of ethanol (50 SCCM and 200 SCCM). The major SWNTs diameters grown with 50 SCCM ethanol flow rate are 0.79 nm (93%) and 1.06 nm (5%). In the case of 200 SCCM flow rate of ethanol, the four major SWNTs diameters (1.10 nm, 1.17 nm, 1.30 nm, and 1.42 nm) are distributed in similar ratio on the surface.

These three RBM frequencies correspond to the diameters of SWNTs in 1.16 nm, 1.06 nm, and 0.79 nm, respectively. The corresponding hyperspectral RBM image (Fig. 3(*c*)) gives a spatial distribution of vertically aligned SWNTs with three different colors (red, green, and blue). The statistical treatment of RBM images can quantify the diameter of SWNTs. In the Raman hyperspectral image, the brightness of each color represents the intensity of the RBM spectrum and the intensity of the RBM peak is closely correlated with the density of SWNTs. Each color represents a group of vertically aligned SWNTs of the same diameter distribution. The blue area in the hyperspectral RBM image (Fig. 3(*c*)) represents a 303 cm^{-1} peak in RBM and the green area corresponds to a 230 cm^{-1} peak. Therefore, all of the SWNTs in the blue and green areas have 0.79 nm and 1.06 nm in a diameter, respectively. Figure 3(*c*) also clearly shows that the diameter distribution of SWNTs is very uniform with blue color. The blue (0.79 nm) and green (1.06 nm) areas occupy over 98% on the surface. In the case of SWNTs grown with 200 SCCM ethanol flow rate, however, the hyperspectral RBM image shows many components of color (Fig. 3(*d*)). They have four major RBM peaks and the peak positions are 174.3 cm^{-1}, 191.1 cm^{-1}, 208.7 cm^{-1}, and 224.7 cm^{-1}. The corresponding diameters of SWNTs are 1.42 nm (174.3 cm^{-1}), 1.30 nm (191.1 cm^{-1}), 1.17 nm (208.7 cm^{-1}), and 1.10 nm (224.7 cm^{-1}). In Fig. 3(*d*), the blue, green, red, and yellow colored regions represent 1.10 nm, 1.17 nm, 1.30 nm, and 1.42 nm diameters of SWNTs, respectively. Also, all these four major SWNT diameters are distributed in a similar portion in the substrate, as shown Fig. 3(*d*). This means that SWNTs grown with 200 SCCM ethanol flow rate have a larger SWNT diameter distribution on the surface than SWNTs synthesized with the 50 SCCM flow rate of ethanol. We have also determined major diameter distributions of vertically aligned SWNTs grown with two different flow rates of ethanol (50 SCCM and 200 SCCM) using peak fitting and integrated band width from each representative RBM spectrum extracted from the RBM mapping process. As shown in Fig. 4, 98% of vertically aligned SWNTs synthesized with a 50 SCCM flow rate of ethanol have diameters in the range 0.79–1.06 nm. However, for SWNTs grown with a 200 SCCM ethanol flow rate, all four different diameters are distributed in similar ratio on the surface.

To scrutinize our experimental observation of the correlation between the SWNT diameter and flow rate of carbon source, we have performed the first-principles density functional theory [17–19] to calculate the diffusion barrier of carbon atoms on the surface of Co catalyst nanoparticles and Al surface, and kinetic Monte Carlo simulations to study the kinetics of carbon nanotube formation on Co catalyst nanoparticles. From our previous work [13], the calculated diffusion barrier of a carbon atom on the Co (001) surface is ~0.15 eV along the minimum barrier path, which connects the face center of a Co triangle, which is the equilibrium position, and the middle of a Co–Co bonding, whereas it is ~1.5 eV through the top of a Co atom [13]. Most carbon atoms will diffuse along the minimum barrier directions. In the case of an Al surface, the diffusion barrier is around 0.1–0.4 eV, but near the boundary of the Co catalyst nanoparticle, the bonding energy of a carbon atom is much higher than those on the Al surface and Co surface. Both the binding energy and the repelling barrier become trap energy of carbon atom to overcome in order to diffuse onto Co catalyst nanoparticles [13].

The differences of carbon source flow rates provide different carbon fluxes on the substrate. Carbon source molecules are dissociated into atoms and smaller molecules at around 850°C (optimum SWNT growth temperature). We assumed only carbon atoms that diffuse on the Al surface to study SWNT nucleation on Co catalyst nanoparticles. While diffusing the carbon source at 850°C, they encounter each other to form carbon aggregations, which also diffuse, but more slowly than a single carbon atom or smaller carbon aggregations. Carbon atoms or carbon aggregations diffuse further until they meet Co catalyst nanoparticles. Since their diffusion on the Al surface is faster than their escaping ratio on the Co perimeter, they are accumulated at the perimeter of Co catalyst nanoparticles. The density of the accumulated carbon at the boundary of Co catalyst nanoparticles is determined by the

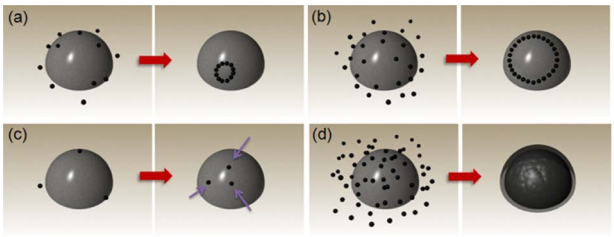

Fig. 5 Schematics of our simple model for SWNT growth with different flow rates: (*a*) and (*b*) shows different flow rates of carbon sources at the Co nanoparticle perimeters, which will make nucleation of carbon nanotubes with different sizes; (*a*) corresponds to the flow rate of 50 SCCM, which makes smaller diameter nanotubes, while (*b*) corresponds to 200 SCCM making larger diameter nanotubes. (*c*) If the flow rate is too low, then collected carbon source at the perimeter of the Co particle is not enough to form a nucleation, so no carbon nanotube would grow. (*d*) In the case of overflow rate, the collected carbon source at the perimeter of the Co nanoparticles covers the surface of Co nanoparticles and the catalyst nanoparticles are deactivated for the growth of SWNTs [13].

carbon flux or the flow rate. Then, aggregations of some carbon atoms at the perimeter enter onto the surface of Co catalyst nanoparticles, while some stay at the perimeter or diffuse out to the Al surface [13]. Figures 5(*a*) and 5(*b*) shows schematics of the different densities of carbon sources at the Co catalyst nanoparticle boundaries, which will make single walled carbon nanotube nucleation with different sizes (different diameters). A different density at the perimeter corresponds to different flow rates of carbon source. As shown Fig. 5(*a*), an ethanol flow rate of 50 SCCM makes smaller diameter single walled carbon nanotubes, while 200 SCCM makes larger nanotubes, as shown in Fig. 5(*b*). Figure 5(*c*) shows that when flow rate is too low, collected carbon source at the perimeter of the Co catalyst nanoparticle is not sufficient to form a nucleation site for a carbon nanotube to grow [13]. On the other hand, if the carbon source flow rate is overflowed, the surface of catalyst nanoparticles is covered with amorphous carbon and they are deactivated (Fig. 5(*d*)).

This paper shows an approach to diameter-selective growth of carbon nanotubes. However, to harness the full potential of CNTs, we also need to control chirality. This remains as a major challenge in facing carbon nanotube synthesis. There is a need for full understanding that will have to include multiscale modeling coupled with experiments to develop a better understanding of the atomic-scale physical and chemical reactions during the nanotube growth process and how to control it. This will only happen if the growth process is completely under control including the thermal and concentration gradients locally at the nanotube scale and globally within the CVD chamber.

4 Conclusion

In conclusion, we have demonstrated the selective growth of vertically aligned SWNTs and DWNTs by controlling the size of catalyst nanoparticles in a highly effective ethanol thermal CVD process. We have also investigated the effect of ethanol flow rate during CVD for the diameter controlled growth of vertically aligned SWNTs by using the Raman RBM mapping process, providing a large-scale spatial diameter distribution of SWNTs. SWNTs synthesized with a lower ethanol flow have a uniform diameter distribution and a smaller diameter compared with that used higher ethanol flow rate. We have also presented a theoretical SWNT growth model under different flow rates of carbon source. From our experimental and theoretical results, it is assumed that a lower flow rate of carbon source makes a smaller nucleation site for a SWNT resulting in a smaller diameter formation. On the other hand, a higher flow rate of carbon source forms a larger nucleation site forming a SWNT with the larger diameter.

Acknowledgment

This work was supported by the Fundamental R&D Program for Core Technology of Materials funded by the Ministry of Knowledge Economy, Republic of Korea and the National Science Foundation (NSF)-Nanoscale Science and Engineering Center (NSF-NSEC) for High-Rate Nanomanufacturing. Y.J.J. also acknowledges Dr. Lijie Ci at Rice University for the TEM characterization.

References

[1] Iijima, S., and Ichihashi, T., 1993, "Single-Shell Carbon Nanotubes of 1-nm Diameter," Nature (London), **363**(6430), pp. 603–605.
[2] Ajayan, P., 1999, "Nanotubes From Carbon," Chem. Rev., **99**(7), pp. 1787–1800.
[3] Graham, A. P., Duesberg, G. S., Seidel, R. V., Liebau, M., Unger, E., Pamler, W., Kreupl, F., and Hoenlein, W., 2005, "Carbon Nanotubes for Microelectronics?," Small, **1**(4), pp. 382–390.
[4] Küttel, O. M., Groening, O., Emmenegger, C., and Schlapbach, L., 1998, "Electron Field Emission From Phase Pure Nanotube Films Grown in a Methane/Hydrogen Plasma," Appl. Phys. Lett., **73**(15), pp. 2113–2115.
[5] Ngo, Q., Cruden, B. A., Cassell, A. M., Sims, G., Meyyappan, M., Li, J., and Yang, C. Y., 2004, "Thermal Interface Properties of Cu-Filled Vertically Aligned Carbon Nanofiber Arrays," Nano Lett., **4**(12), pp. 2403–2407.
[6] Cheng, H., Li, F., Sun, X., Brown, S., Pimenta, M., Marucci, A., Dresselhaus, G., and Dresselhaus, M., 1998, "Bulk Morphology and Diameter Distribution of Single-Walled Carbon Nanotubes Synthesized by Catalytic Decomposition of Hydrocarbons," Chem. Phys. Lett., **289**(5–6), pp. 602–610.
[7] Ci, L., Xie, S., Tang, D., Yan, X., Li, Y., Liu, Z., Zou, X., Zhou, W., and Wang, G., 2001, "Controllable Growth of Single Wall Carbon Nanotubes by Pyrolizing Acetylene on the Floating Iron Catalysts," Chem. Phys. Lett., **349**(3–4), pp. 191–195.
[8] Colomer, J., Benoit, J., Stephan, C., Lefrant, S., Van Tendeloo, G., and Nagy, J. B., 2001, "Characterization of Single-Wall Carbon Nanotubes Produced by CCVD Method," Chem. Phys. Lett., **345**(1–2), pp. 11–17.
[9] Colomer, J., Stephan, C., Lefrant, S., Van Tendeloo, G., Willems, I., Kónya, Z., Fonseca, A., Laurent, C., and Nagy, J., 2000, "Large-Scale Synthesis of Single-Wall Carbon Nanotubes by Catalytic Chemical Vapor Deposition (CCVD) Method," Chem. Phys. Lett., **317**(1–2), pp. 83–89.
[10] Nikolaev, P., Bronikowski, M., Bradley, R., Rohmund, F., Colbert, D., Smith, K., and Smalley, R., 1999, "Gas-Phase Catalytic Growth of Single-Walled Carbon Nanotubes From Carbon Monoxide," Chem. Phys. Lett., **313**(1–2), pp. 91–97.
[11] Satishkumar, B., Govindaraj, A., Sen, R., and Rao, C., 1998, "Single-Walled Nanotubes by the Pyrolysis of Acetylene-Organometallic Mixtures," Chem. Phys. Lett., **293**(1–2), pp. 47–52.
[12] Zhou, W., Ooi, Y., Russo, R., Papanek, P., Luzzi, D., Fischer, J., Bronikowski, M., Willis, P., and Smalley, R., 2001, "Structural Characterization and Diameter-Dependent Oxidative Stability of Single Wall Carbon Nanotubes Synthesized by the Catalytic Decomposition of Co," Chem. Phys. Lett., **350**(1–2), pp. 6–14.
[13] Hahm, M. G., Kwon, Y.-K., Lee, E., Ahn, C. W., and Jung, Y. J., 2008, "Diameter Selective Growth of Vertically Aligned Single Walled Carbon Nanotubes and Study on Their Growth Mechanism," J. Phys. Chem. C, **112**(44), pp. 17143–17147.
[14] Murakami, Y., Chiashi, S., Miyauchi, Y., Hum, M., Ogura, M., Okubo, T., and Maruyama, S., 2004, "Growth of Vertically Aligned Single-Walled Carbon Nanotube Films on Quartz Substrates and Their Optical Anisotropy," Chem. Phys. Lett., **385**, pp. 298–303.
[15] Hata, K., Futaba, D. N., Mizuno, K., Namai, T., Yumura, M., and Iijima, S., 2004, "Water-Assisted Highly Efficient Synthesis of Impurity-Free Single-Walled Carbon Nanotubes," Science, **306**, pp. 1362–1364.
[16] Jorio, A., Pimenta, M. A., Souza Filho, A. G., Saito, R., Dresselhaus, G., and Dresselhaus, M. S., 2003, "Characterizing Carbon Nanotube Samples With Resonance Raman Scattering," New J. Phys., **5**, pp. 139.1–139.17.
[17] Ihm, J., Zunger, A., and Cohen, M. L., 1980, "Momentum-Space Formalism for the Total Energy of Solids," J. Phys. C, **13**, pp. 3095.
[18] Kohn, W. and Sham, L., 1965, "Self-Consistent Equations Including Exchange and Correlation Effects," Phys. Rev., **140**, pp. A1133–A1138.
[19] Payne, M. C., Teter, M. P., Allan, D. C., Arias, T. A., and Joannopoulos, J. D., 1992, "Iterative Minimization Techniques for Ab Initio Total-Energy Calculations: Molecular Dynamics and Conjugate Gradients," Rev. Mod. Phys., **64**, pp. 1045–1097.